Equivalent in-plane elastic properties of irregular honeycombs: An analytical approach

T. Mukhopadhyay*, S. Adhikari

College of Engineering, Swansea University, Singleton Park, Swansea SA2 8PP, UK

ABSTRACT

An analytical formulation has been developed in this article for predicting the equivalent elastic properties of irregular honeycombs with spatially random variations in cell angles. Employing unit-cell based approaches, closed-form expressions of equivalent elastic properties of regular honeycombs are available. Closed-form expressions for equivalent elastic properties of irregular honeycombs are very scarce in available literature. In general, direct numerical simulation based methods are prevalent for this case. This paper proposes a novel analytical framework for predicting equivalent in-plane elastic moduli of irregular honeycombs using a representative unit cell element (RUCE) approach. Using this approach, closed-form expressions of equivalent in-plane elastic moduli (longitudinal and transverse Young's modulus, shear modulus, Poisson's ratios) have been derived. The expressions of longitudinal Young's modulus, transverse Young's modulus, and shear modulus are functions of both structural geometry and material properties of irregular honeycombs, while the Poisson's ratios depend only on structural geometry of irregular honeycombs. The elastic moduli obtained for different degree of randomness following the proposed analytical approach are found to have close proximity to direct finite element simulation results.

© 2015 Elsevier Ltd. All rights reserved.

1. Introduction

Honeycombs have gained considerable attention in recent years as an advanced material due to its capability of meeting high performance requirements in various critically desirable application-specific parameters. These include specific strength and stiffness, electro-mechanical properties, acoustic properties, shock absorption, fatigue strength, corrosion and fire resistance. Such lattice and/or lattice-like structures are present in materials and structures across different length-scales. The use of honeycomb core in several applications of sandwich structures is an important area of research (Yongqiang and Zhiqiang, 2008; Zenkert, 1995). An in-depth analysis of the structural behavior of honeycomb can be useful in emerging research areas such as carbon nano-materials like graphene, as these are generally idealized to have hexagonal periodic structural forms (Liu et al., 2012; Pantano et al., 2004; Scarpa et al., 2009).

Honeycombs are modeled as a continuous solid having an equivalent elastic moduli throughout its domain. This approach

eliminates the need of detail finite element modeling of honeycombs in complex structural systems like sandwich structures. To date, extensive amount of research has been carried out to predict the equivalent elastic properties of regular honeycombs consisting of perfectly periodic hexagonal cells (El-Sayed et al., 1979; Gibson and Ashby, 1999; Goswami, 2006; Zhang and Ashby, 1992). Constitutive models for two-dimensional linear as well as non-linear elastic foams have been developed in (Warren and Kraynik, 1987) and (Warren et al., 1989) respectively considering an appropriate representative volume element to analyse periodic foam structure. Elasto-plastic yield limits and failure surfaces for large deformations of transversely crushed honeycombs have been analyzed using theoretical predictions in (Klintworth and Stronge, 1988). Recently numerical investigations of buckling and crushing behavior of expanded honeycomb are found to be carried out by Jang and Kyriakides (2015), while Wilbert et al. (2011) have studied buckling and progressive crushing of laterally loaded honeycombs. Other important research areas concerning the study of different responses related to periodic honeycombs include low velocity impact (Hu and Yu, 2013) and buckling analysis (Lopez Jimenez and Triantafyllidis, 2013) and wave propagation through lattices (Schaeffer and Ruzzene, 2015). There is a substantial amount of literature available on the study of perfectly periodic hexagonal auxetic honeycombs (Critchley et al., 2013; Rossiter et al., 2014; Scarpa et al., 2000). Of late theoretical formulations for equivalent elastic properties of periodic asymmetrical honeycomb have been

---

developed in (Chen and Yang, 2011), while the tailorable properties of hierarchical honeycombs, including spiderweb honeycombs have been investigated in (Ajdari et al., 2012; Mousanezhad et al., 2015). Analysis of two dimensional honeycombs dealing with in-plane elastic properties presented in the above survey are commonly based on unit cell approach, which is applicable only for perfectly periodic cellular structures.

A significant limitation of the aforementioned unit cell approach is that it cannot account for the spatial irregularity, which is practically inevitable. Spatial irregularity in honeycomb may occur due to manufacturing uncertainty, structural defects, variation in temperature, pre-stressing and micro-structural variability in honeycombs. To include the effect of irregularity, voronoi honeycombs have been considered in several studies (Li et al., 2005; Zhu et al., 2001; 2006). Dynamic crushing behavior of honeycomb structures with irregularity in cell shapes and cell wall thickness have been investigated in (Li et al., 2007). Triantafyllidis and Schraad (1998) have reported study on failure surface of aluminium honeycombs under general in-plane loading to compare the theoretical results, obtained for the infinite, perfectly periodic honeycomb model and the numerical results, obtained for the finite counterpart with micro-structural imperfections considering uncertainties in manufacturing and fabrication. Jang and Kyriakides (2015); Papka and Kyriakides (1994); 1998) carried out numerical and experimental study of honeycomb buckling and crushing behavior considering geometrical imperfections in the structure such as variation in length of bond line and over or under expanded cells. Though these studies substantially explore the effect of imperfections as pioneering works, a further need is felt to extend these works for spatially random imperfections to develop more realistic model of the uncertainties associated with such irregularities. Stochastic multi-scale analysis for the elastic properties of honeycombs have been presented in more recent studies (Basaruddin et al., 2014). The effect of defects on the behavior of regular as well as voronoi honeycombs (Ajdari et al., 2008), and the effect of manufacturing irregularity on auxetic honeycomb (Liu et al., 2014) have been investigated. In the studies involving voronoi honeycombs, the shape of all irregular cells generated using voronoi diagram may not be necessarily hexagonal, which violates the presumption of hexagonal cell structure in many applications. Published researches that explore the effect of different forms of irregularity on elastic properties and structural responses of honeycombs are based on either experimental investigations or expensive finite element (FE) simulation. Experimental investigations, being very expensive and time consuming, its practically not feasible to capture the effect of random irregularities in honeycomb structure by testing huge number of samples. In finite element approach, a small change in geometry of a single cell may require completely new geometry and meshing of the entire structure. In general this makes the entire process time-consuming and tedious. For quasi-static and dynamic analysis, finite element modeling of the cellular core in a sandwich panel may increase the degree of freedom of the entire structure up to huge extent, making the overall process more complex and prohibitively expensive to simulate. The problem becomes even worse for uncertainty quantification of the responses associated with irregular honeycombs, where the expensive finite element model is needed to be simulated for a large number of samples while using a Monte Carlo based approach (Dey et al., 2015a; 2015b; 2015c; Hurtado and Barbat, 1998). Direct numerical simulation to deal with irregularity in honeycombs may not necessarily provide proper understanding of the underlying physics of the system. An analytical approach could be a simple, insightful, yet an efficient way to obtain effective elastic properties of honeycombs.

This paper develops an analytical framework for predicting equivalent in-plane elastic properties of irregular honeycomb having spatially random variations in cell angle. Geometrical imperfections due to over or under expanded cells have been considered by Papka and Kyriakides (1994). However, random spatial distribution of over or under expanded cells has not been considered yet, which can be a realistic and logical extension of the previous work. As this article proposes closed-form formulae for such irregularities, the responses can be investigated in a more robust but efficient manner. Towards the development of explicit analytical formulae of in-plane elastic moduli for addressing any such form of irregularity in cellular structures, this is the first attempt of its kind to the best of authors' knowledge. closed-form formulae developed here can be a computationally efficient and less-tedious alternative to the expensive finite element modeling and simulation approach for many applications. This article is organized as follows. Derivations of formulae for five in-plane elastic moduli of irregular honeycombs are described in Section 2. Development of finite element model to obtain the in-plane elastic moduli numerically and validation of the finite element code with available literature (Gibson and Ashby, 1999) are discussed in Section 3. Variations of elastic moduli for different degree of random variations in the cell angle and comparison of results between the proposed analytical approach and finite element simulation are detailed in Section 4. Finally, Section 5 summarises the main findings and draws conclusions based on the results obtained in the paper.

2. Elastic properties of irregular honeycombs

The key idea to obtain the effective in-plane elastic moduli of the entire irregular honeycomb structure is that it is considered to be consisted of several representative unit cell elements having different individual elastic moduli. Elastic properties of each representative unit cell element (RUCE) depends on its structural geometry and material properties. The irregularity is accounted implicitly by means of the RUCEs. The RUCE considered in this study for deriving the expressions of different in-plane elastic moduli for an irregular honeycomb structure is shown in Fig. 1(b). The expressions for elastic moduli of a RUCE is derived first and subsequently the expressions for effective in-plane elastic moduli of the entire irregular honeycomb are derived by assembling the individual elastic moduli of these RUCEs using basic principles of mechanics as discussed in the preceding sections. These formulae are applicable for both tensile as well as compressive stresses.

2.1. Longitudinal Young's modulus (E_1)

To derive the expression of longitudinal Young's modulus for a RUCE (E_{1U}), stress σ_1 is applied in direction-1 (refer figure Fig. 1) as shown in Fig. 2. The inclined cell walls having inclination angle α and β do not have any contribution in the analysis, as the stresses applied on them in two opposite directions neutralise each other. The remaining structure except these two inclined cell walls is symmetric. The applied stresses cause the inclined cell walls having inclination angle θ to bend. From the condition of equilibrium, the vertical forces C in the free-body diagram of these cell walls (refer Fig. 2(b)) need to be zero. In the present analysis the cell walls are treated as beams of thickness t, depth b and Young's modulus E_s. l and h are the lengths of inclined cell walls having inclination angle θ and the vertical cell walls respectively. From Fig. 2(b),

$$M = \frac{Pl\sin\theta}{2} \tag{1}$$

where

$$P = \sigma_1(h + l\sin\theta)b \tag{2}$$

From the standard beam theory (Roark and Young, 1976), the deflection of one end compared to the other end of the cell wall

(a) regular honeycomb   (b) irregular honeycomb
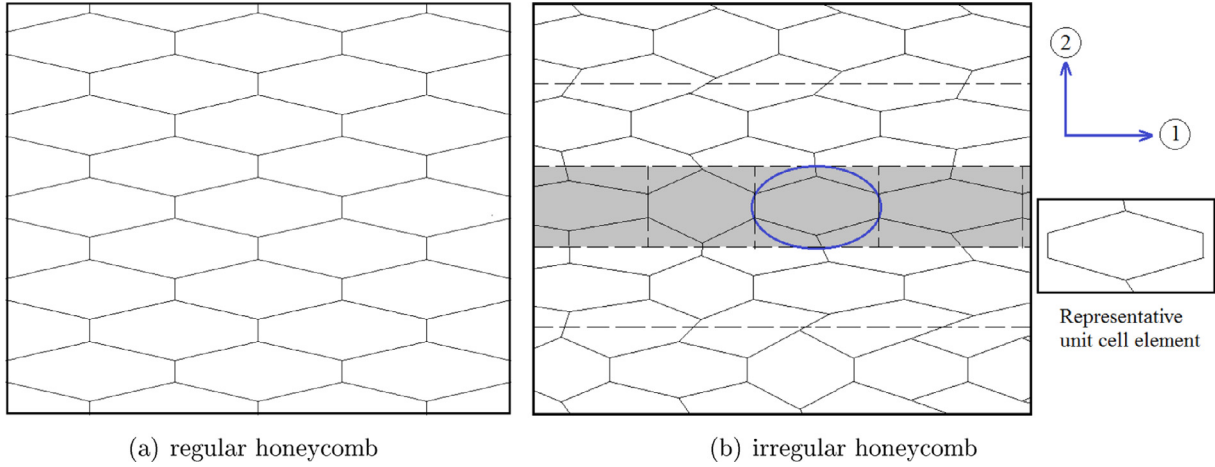
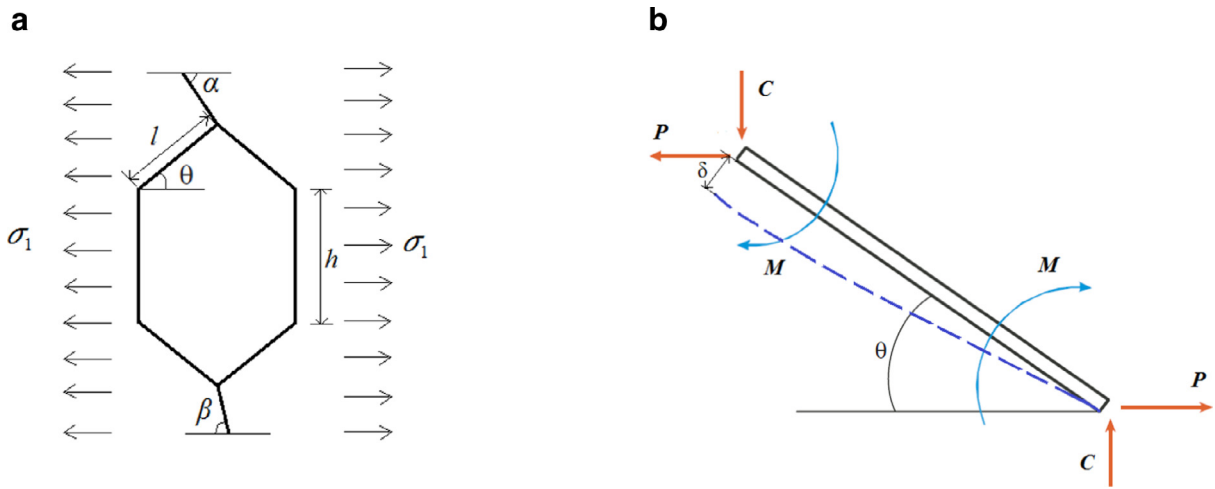**Fig. 1.** Typical representation of regular and irregular honeycomb structure.

Fig. 2. RUCE and free-body diagram used in the proposed analysis for E_1.

shown in Fig. 2(b) can be expressed as

$$\delta = \frac{Pl^3 \sin\theta}{12 E_s I} \tag{3}$$

where I is the second moment of inertia of the cell wall, that is $I = bt^3/12$.

The component of δ parallel to direction-1 is $\delta\sin\theta$. The strain parallel to direction-1 becomes

$$\epsilon_1 = \frac{\delta \sin\theta}{l \cos\theta} \tag{4}$$

Thus the Young's modulus in direction-1 for a RUCE can be expressed as

$$E_{1U} = \frac{\sigma_1}{\epsilon_1} = E_s \left(\frac{t}{l}\right)^3 \frac{\cos\theta}{\left(\frac{h}{l} + \sin\theta\right) \sin^2\theta} \tag{5}$$

To derive the expression of equivalent Young's modulus in direction-1 for the entire irregular honeycomb structure (E_{1eq}), the Young's moduli for the constituting RUCEs (E_{1U}) are assembled as discussed next. In the present analysis, the entire irregular honeycomb structure (Fig. 1(b)) is assumed to have m and n number of RUCEs in direction-1 and direction-2 respectively. A particular cell having position at ith column and jth row is represented as (i, j), where $i = 1, 2, \ldots, m$ and $j = 1, 2, \ldots, n$. To obtain E_{1eq}, stress σ_1 is applied in direction-1 as shown in Fig. 3(a). If the deformation compatibility condition of jth strip (as highlighted in Fig. 1(b)) is

considered, the total deformation due to stress σ_1 of that particular strip (Δ_1) is the summation of individual deformations of each RUCEs in direction-1, while deformation of each of these RUCEs in direction-2 is same. Thus for the jth strip

$$\Delta_1 = \sum_{i=1}^{m} \Delta_{1ij} \tag{6}$$

The Eq. (6) can be rewritten as

$$\epsilon_1 L = \sum_{i=1}^{m} \epsilon_{1ij} L_{ij} \tag{7}$$

where ϵ_1 and L represent strain and dimension in direction-1 of respective elements. Eq. (7) leads to

$$\frac{\sigma_1 L}{\hat{E}_{1j}} = \sum_{i=1}^{m} \frac{\sigma_1 L_{ij}}{E_{1Uij}} \tag{8}$$

From Eq. (8), equivalent Young's modulus of jth strip ($\hat{E}_{1j}$) can be expressed as

$$\hat{E}_{1j} = \frac{\sum_{i=1}^{m} l_{ij} \cos\theta_{ij}}{\sum_{i=1}^{m} \frac{l_{ij} \cos\theta_{ij}}{E_{1Uij}}} \tag{9}$$

where θ_{ij} is the inclination angle of the cell walls having length l_{ij} in the RUCE positioned at (i, j).

(a) Entire idealized irregular honeycomb structure

(b) Idealized j^{th} strip

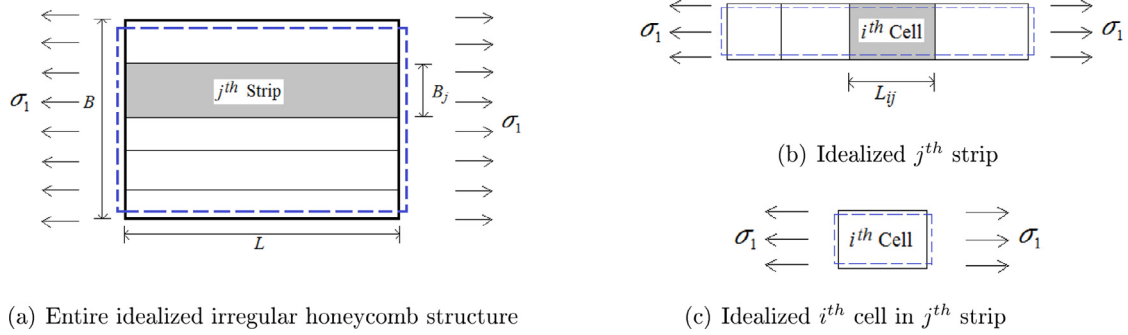(c) Idealized i^{th} cell in j^{th} strip

Fig. 3. Free-body diagrams of idealized irregular honeycomb structure in the proposed analysis of E_1.
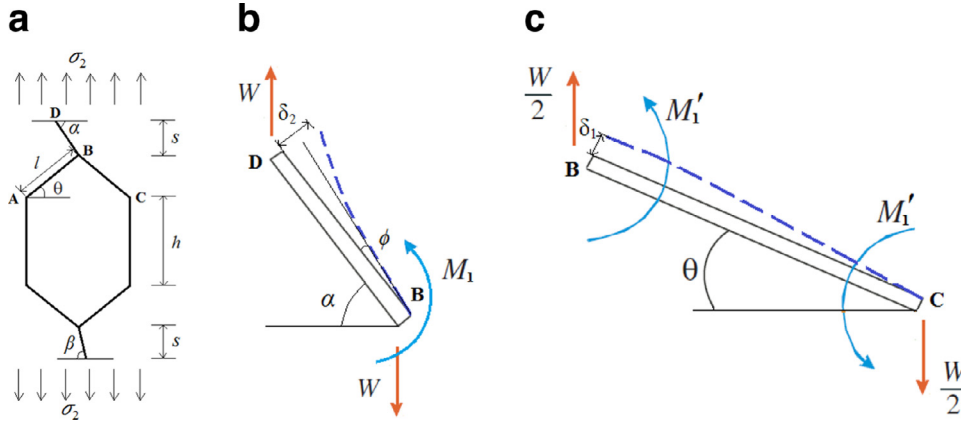

Fig. 4. RUCE and free-body diagram used in the proposed analysis for E_2.

After obtaining the Young's moduli of n number of strips, they are assembled to achieve the equivalent Young's modulus of the entire irregular honeycomb structure (E_{1eq}) using force equilibrium and deformation compatibility conditions.

$$\sigma_1 Bb = \sum_{j=1}^{n} \sigma_{1j} B_j b \tag{10}$$

where B_j is the dimension of jth strip in direction-2 and $B = \sum_{j=1}^{n} B_j$. b represents the depth of honeycomb. As strains in direction-1 for each of the n strips are same to satisfy the deformation compatibility condition, Eq. (10) leads to

$$\left(\sum_{j=1}^{n} B_j\right) E_{1eq} = \sum_{j=1}^{n} \hat{E}_{1j} B_j \tag{11}$$

Using Eqs. (9) and (11), equivalent Young's modulus in direction-1 of the entire irregular honeycomb structure (E_{1eq}) can be expressed as

$$E_{1eq} = \frac{1}{\sum_{j=1}^{n} B_j} \sum_{j=1}^{n} \left(\frac{\sum_{i=1}^{m} l_{ij} \cos\theta_{ij}}{\sum_{i=1}^{m} \frac{l_{ij} \cos\theta_{ij}}{E_{1Uij}}}\right) B_j \tag{12}$$

where Young's modulus in direction-1 of a RUCE positioned at (i, j) is E_{1Uij}, which can be obtained from Eq. (5).

2.2. Transverse Young's modulus (E_2)

To derive the expression of transverse Young's modulus for a RUCE (E_{2U}), stress σ_2 is applied in direction-2 (refer Fig. 1) as shown in Fig. 4(a). Total deformation of the RUCE in direction-2 consists of three components, namely deformation of the cell wall having inclination angle α, deformation of the cell walls having inclination angle θ and deformation of the cell wall having inclination angle β. All the cell walls are considered axially rigid in this analysis. If the remaining structure except the two inclined cell walls having inclination angle α and β is considered, two forces that act at joint B are W and M_1. For the cell wall having inclination angle α, effect of the bending moment M_1 generated due to application of W at point D is only to create rotation (ϕ) at the joint B.

Vertical deformation of the cell wall having inclination angle α has two components, bending deformation in direction-2 and rotational deformation due the rotation of joint B as shown in Fig. 4(b). The bending deformation in direction-2 can be expressed as

$$\delta_{2vb} = \left(\frac{W\cos\alpha \left(\frac{s}{\sin\alpha}\right)^3}{3E_s I}\right) \cos\alpha \tag{13}$$

where $W = 2\sigma_2 lb\cos\theta$ and $I = bt^3/12$.

From Fig. 4(b), $M_1 = W\scot\alpha$. Cell walls BC and BA will share half of moment M_1 each as they have equal stiffness. Using the standard result of Euler–Bernoulli beam theory, deflection at one end due to application of moment at the other end ($\delta = Ml^2/6E_s I$), the angle of rotation at joint B can be expressed as

$$\phi = \frac{M_1}{2} \frac{l}{6E_s I} \tag{14}$$

The component of rotational deformation of the cell wall having inclination angle α in direction-2 can be expressed as

$$\delta_{2vr} = \phi\left(\frac{s}{\sin\alpha}\right)\cos\alpha \tag{15}$$

Thus from Eqs. (13)–(15) after replacing $W = 2\sigma_2 lb\cos\theta$, $M_1 = W\scot\alpha$ and $I = bt^3/12$, total deformation in direction-2 of the cell

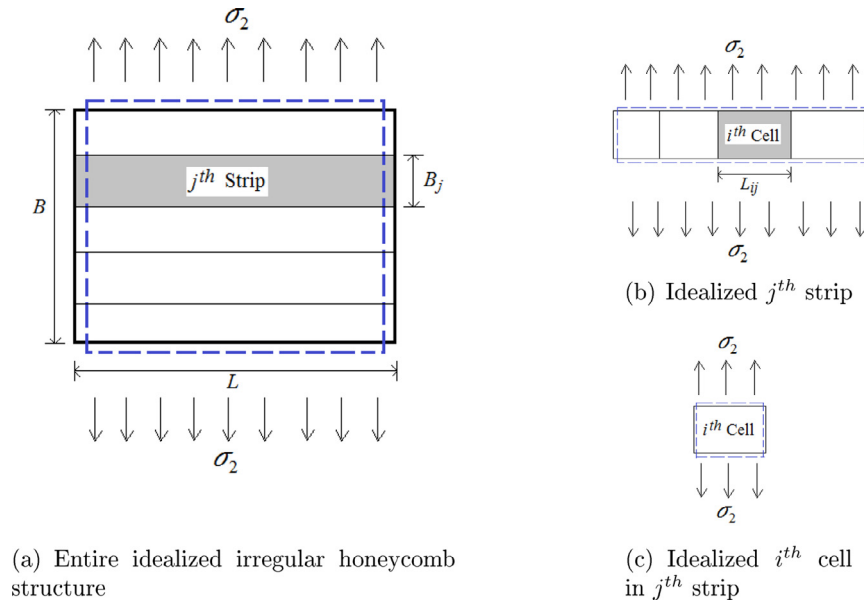(a) Entire idealized irregular honeycomb structure

(b) Idealized j^{th} strip

(c) Idealized i^{th} cell in j^{th} strip

Fig. 5. Free-body diagrams of idealized irregular honeycomb structure in the proposed analysis of E_2.

wall having inclination angle α can be expressed as

$$\delta_{v2} = \delta_{2vb} + \delta_{2vr} = \frac{2\sigma_2 s^2 l \cos\theta}{E_s t^3}\left(4s\frac{\cos^2\alpha}{\sin^3\alpha} + l\cot^2\alpha\right) \quad (16)$$

Deformation in direction-2 of the cell wall having inclination angle β can also be expressed in the similar way as

$$\dot{\delta}_{v2} = \frac{2\sigma_2 s^2 l \cos\theta}{E_s t^3}\left(4s\frac{\cos^2\beta}{\sin^3\beta} + l\cot^2\beta\right) \quad (17)$$

From Fig. 4(c), deformation of each of the cell walls having inclination angle θ in direction-2

$$\bar{\delta}_{v1} = \frac{(\frac{W}{2}\cos\theta)l^3}{12E_s I}\cos\theta \quad (18)$$

Replacing $W = 2\sigma_2 lb\cos\theta$ and $I = bt^3/12$ from Eq. (18), total deformation in direction-2 of two cell walls having inclination angle θ can be expressed as

$$\delta_{v1} = \frac{2\sigma_2 l^4 \cos^3\theta}{12E_s t^3} \quad (19)$$

Thus total deformation in direction-2 of the RUCE represented in Fig. 4(a) due to application of stresses σ_2 is

$$\begin{aligned}\delta_v &= \delta_{v2} + \dot{\delta}_{v2} + \delta_{v1} \\ &= \frac{\sigma_2 l \cos\theta}{E_s t^3}\left(2l^3\cos^2\theta + 8s^3\left(\frac{\cos^2\alpha}{\sin^3\alpha} + \frac{\cos^2\beta}{\sin^3\beta}\right)\right. \\ &\quad\left. + 2s^2 l(\cot^2\alpha + \cot^2\beta)\right)\end{aligned} \quad (20)$$

Strain in direction-2 can be obtained as

$$\epsilon_2 = \frac{\delta_v}{h + 2s + 2l\sin\theta} \quad (21)$$

Thus Young's modulus in direction-2 of a RUCE can be expressed as

To derive the expression of equivalent Young's modulus in direction-2 for the entire irregular honeycomb structure (E_{2eq}), the Young's moduli for the constituting RUCEs (E_{2U}) are assembled as discussed below. For obtaining E_{2eq}, stress σ_2 is applied in direction-2 as shown in Fig. 5(a)). If the force equilibrium under the application of stress σ_2 of jth strip (as highlighted in Fig. 5(b)) is considered,

$$\sigma_2\left(\sum_{i=1}^{m}2l_{ij}\cos\theta_{ij}\right)b = \left(\sum_{i=1}^{m}\sigma_{2ij}2l_{ij}\cos\theta_{ij}\right)b \quad (23)$$

By deformation compatibility condition, strains of each RUCE in direction-2 of the jth strip are same. Eq.(23), rewritten as

$$\hat{E}_{2j}\left(\sum_{i=1}^{m}l_{ij}\cos\theta_{ij}\right)\epsilon = \left(\sum_{i=1}^{m}E_{2Uij}l_{ij}\cos\theta_{ij}\epsilon_{ij}\right) \quad (24)$$

where $\epsilon_{ij} = \epsilon$, for $i = 1, 2\ldots m$ in the jth strip. $\hat{E}_{2j}$ is the equivalent elastic modulus in direction-2 of the jth strip.

$$\hat{E}_{2j} = \frac{\sum_{i=1}^{m}E_{2Uij}l_{ij}\cos\theta_{ij}}{\sum_{i=1}^{m}l_{ij}\cos\theta_{ij}} \quad (25)$$

Total deformation of the entire honeycomb in direction-2 (Δ_2) is the sum of deformations of each strips in that direction,

$$\Delta_2 = \sum_{j=1}^{n}\Delta_{2ij} \quad (26)$$

The Eq. (26) can be rewritten as

$$\epsilon_2 B = \sum_{j=1}^{n}\epsilon_{2j}B_j \quad (27)$$

where ϵ_2, ϵ_{2j} and B_j represent total strain of the entire honeycomb structure in direction-2, strain of jth strip in direction-2 and

$$E_{2U} = \frac{\sigma_2}{\epsilon_2} = E_s\left(\frac{t}{l}\right)^3\frac{(\frac{h}{l} + 2\frac{s}{l} + 2\sin\theta)}{\cos\theta(2\cos^2\theta + 8(\frac{s}{l})^3(\frac{\cos^2\alpha}{\sin^3\alpha} + \frac{\cos^2\beta}{\sin^3\beta}) + 2(\frac{s}{l})^2(\cot^2\alpha + \cot^2\beta))} \quad (22)$$

dimension in direction-2 of *j*th strip respectively. Eq. (27) can be rewritten as

$$\frac{\sigma_2 \sum_{j=1}^{n} B_j}{E_{2eq}} = \sum_{j=1}^{n} \frac{\sigma_2 B_j}{\hat{E}_{2j}} \tag{28}$$

From Eqs. (25) and (28), the Young's modulus in direction-2 of the entire irregular honeycomb structure can be expressed as

$$E_{2eq} = \frac{1}{\left(\sum_{j=1}^{n} B_j \frac{\sum_{i=1}^{m} l_{ij} \cos\theta_{ij}}{\sum_{i=1}^{m} E_{2Uij} l_{ij} \cos\theta_{ij}}\right)} \sum_{j=1}^{n} B_j \tag{29}$$

where Young's modulus in direction-2 of a RUCE positioned at (*i, j*) is E_{2Uij}, which can be obtained from Eq. (22).

It is worthy to mention here that the derived expressions of Young's moduli for irregular honeycombs (Eqs. (12) and (29)) can be reduced to the formulae provided by Gibson and Ashby (Gibson and Ashby, 1999) in case of uniform honeycombs (i.e. $B_1 = B_2 = \cdots = B_n$; $s = h/2$; $\alpha = \beta = 90°$; $l_{ij} = l$ and $\theta_{ij} = \theta$, for all *i* and *j*). By applying the conditions $B_1 = B_2 = \cdots = B_n$; $l_{ij} = l$ and $\theta_{ij} = \theta$, Eqs. (12) and (29) reduce to E_{1U} and E_{2U} respectively. For $s = h/2$ and $\alpha = \beta = 90°$, E_{1U} and E_{2U} produce the same expressions for Young's moduli of uniform honeycomb as presented by Gibson and Ashby (Gibson and Ashby, 1999). In case of regular uniform honeycombs ($\theta = 30°$)

$$\frac{E_1^*}{E_s} = \frac{E_2^*}{E_s} = 2.3\left(\frac{t}{l}\right)^3 \tag{30}$$

where E_1^* and E_2^* denote the Young moduli of uniform regular honeycombs in longitudinal and transverse direction respectively.

2.3. Poisson's ratio ν_{12}

Poisson's ratios are calculated by taking the negative ratio of strains normal to, and parallel to, the loading direction. Poisson's ratio of a RUCE for the loading direction-1 (ν_{12U}) is obtained as (refer Fig. 2(a))

$$\nu_{12U} = -\frac{\epsilon_2}{\epsilon_1} \tag{31}$$

where ϵ_1 and ϵ_2 represent the strains of a RUCE in direction-1 and direction-2 respectively due to loading in direction-1. ϵ_1 can be obtained from Eq. (4). From Fig. 2(b), ϵ_2 can be expressed as

$$\epsilon_2 = -\frac{2\delta \cos\theta}{h + 2l\sin\theta + 2s} \tag{32}$$

Thus the expression for Poisson's ratio of a RUCE for the loading direction-1 becomes

$$\nu_{12U} = \frac{2\cos^2\theta}{(2\sin\theta + 2\frac{s}{l} + \frac{h}{l})\sin\theta} \tag{33}$$

To derive the expression of equivalent Poisson's ratio for loading direction-1 of the entire irregular honeycomb structure (ν_{12eq}), the Poisson's ratios for the constituting RUCEs (ν_{12U}) are assembled as discussed below. For obtaining ν_{12eq}, stress σ_1 is applied in direction-1 as indicated in Fig. 3(a)). If the application of stress σ_1 in the *j*th strip (as highlighted in Fig. 3(b)) is considered, total deformation of the *j*th strip in direction-1 is summation of individual deformations of the RUCEs in direction-1 of that particular strip. Thus from Eq. (7), using the basic definition of ν_{12},

$$-\frac{\epsilon_2}{\hat{\nu}_{12j}} L = -\sum_{i=1}^{m} \frac{\epsilon_{2ij} L_{ij}}{\nu_{U12ij}} \tag{34}$$

where ϵ_2 and ϵ_{2ij} are the strains in direction-2 of *j*th strip and individual RUCEs of *j*th strip respectively. ν_{U12ij} represents the Poisson's ratio for loading direction-1 of a RUCE positioned at (*i, j*). $\hat{\nu}_{12j}$

denotes the equivalent Poisson's ratio for loading direction-1 of the *j*th strip.

To ensure the deformation compatibility condition $\epsilon_2 = \epsilon_{2ij}$ for $i = 1, 2, \ldots, m$ in the *j*th strip. Thus Eq. (34) leads to

$$\hat{\nu}_{12j} = \frac{L}{\sum_{i=1}^{m} \frac{L_{ij}}{\nu_{12Uij}}} \tag{35}$$

Total deformation of the entire honeycomb structure in direction-2 under the application of stress σ_1 along the two opposite edges parallel to direction-2 is summation of the individual deformations in direction-2 of *n* number of strips. Thus

$$\epsilon_2 B = \sum_{j=1}^{n} \epsilon_{2j} B_j \tag{36}$$

Using the basic definition of ν_{12} Eq. (36) becomes

$$\nu_{12eq} \epsilon_1 B = \sum_{j=1}^{n} \nu_{12j} \epsilon_{1j} B_j \tag{37}$$

where ν_{12eq} represents the equivalent Poisson's ratio for loading direction-1 of the entire irregular honeycomb structure. ϵ_1 and ϵ_{1j} denote the strain of entire honeycomb structure in direction-1 and strain of *j*th strip in direction-1 respectively. From the condition of deformation comparability $\epsilon_1 = \epsilon_{1j}$ for $j = 1, 2, \ldots, n$. Thus from Eqs. (35) and (37),

$$\nu_{12eq} = \frac{1}{\sum_{j=1}^{n} B_j} \sum_{j=1}^{n} \left(\frac{\sum_{i=1}^{m} l_{ij}\cos\theta_{ij}}{\sum_{i=1}^{m} \frac{l_{ij}\cos\theta_{ij}}{\nu_{12Uij}}}\right) B_j \tag{38}$$

where ν_{12Uij} can be obtained from Eq. (33).

2.4. Poisson's ratio ν_{21}

Poisson's ratio of a RUCE for the loading direction-2 (ν_{21U}) is obtained as (refer Fig. 4(a))

$$\nu_{21U} = -\frac{\epsilon_1}{\epsilon_2} \tag{39}$$

where ϵ_1 and ϵ_2 represent the strains of a RUCE in direction-1 and direction-2 respectively due to loading in direction-2. ϵ_2 can be obtained from Eqs. (20) and (21) as

$$\epsilon_2 = \frac{\sigma_2 l \cos\theta}{E_s t^3 (h + 2s + 2l\sin\theta)}$$
$$\times \left(2l^3\cos^2\theta + 8s^3\left(\frac{\cos^2\alpha}{\sin^3\alpha} + \frac{\cos^2\beta}{\sin^3\beta}\right)\right.$$
$$\left. + 2s^2 l(\cot^2\alpha + \cot^2\beta)\right) \tag{40}$$

From Fig. 4(c)

$$\epsilon_1 = -\frac{\delta_1 \sin\theta}{l\cos\theta} \tag{41}$$

where $\delta_1 = \frac{(\frac{W}{2}\cos\theta)l^3}{12E_s I}$ and $W = 2\sigma_2 lb\cos\theta$. Thus Eq. (41) reduces to

$$\epsilon_1 = -\frac{\sigma_2 l^3 \sin\theta\cos\theta}{E_s t^3} \tag{42}$$

Thus the expression for Poisson's ratio of a RUCE for the loading direction-2 becomes

$$\nu_{21U} = \frac{\sin\theta(\frac{h}{l} + 2\frac{s}{l} + 2\sin\theta)}{2\cos^2\theta + 8(\frac{s}{l})^3(\frac{\cos^2\alpha}{\sin^3\alpha} + \frac{\cos^2\beta}{\sin^3\beta}) + 2(\frac{s}{l})^2(\cot^2\alpha + \cot^2\beta)} \tag{43}$$

To derive the expression of equivalent Poisson's ratio for loading direction-2 of the entire irregular honeycomb structure (v_{21eq}), the Poisson's ratios for the constituting RUCEs (v_{21U}) are assembled as discussed below. For obtaining v_{21eq}, stress σ_2 is applied in direction-2 as shown in Fig. 5(a)). If the application of stress σ_2 in the jth strip (as highlighted in Fig. 5(b)) is considered, total deformation of the jth strip in direction-1 is summation of individual deformations of the RUCEs in direction-1 of that particular strip. Thus,

$$\epsilon_1 L = \sum_{i=1}^{m} \epsilon_{1ij} L_{ij} \tag{44}$$

Using the basic definition of v_{21} Eq. (44) leads to

$$\hat{v}_{21j} \epsilon_2 L = \sum_{i=1}^{m} v_{21Uij} \epsilon_{2ij} L_{ij} \tag{45}$$

where $\hat{v}_{21j}$ represents the equivalent Poisson's ratio for loading direction-2 of the jth strip. ϵ_2 and ϵ_{2ij} are the strains in direction-2 of jth strip and individual RUCEs of jth strip respectively. v_{21Uij} represents the Poisson's ratio for loading direction-2 of a RUCE positioned at (i, j).

To ensure the deformation compatibility condition $\epsilon_2 = \epsilon_{2ij}$ for $i = 1, 2, \ldots, m$ in the jth strip. Thus Eq. (45) leads to

$$\hat{v}_{21j} = \frac{\sum_{i=1}^{m} v_{21Uij} l_{ij} \cos\theta_{ij}}{\sum_{i=1}^{m} l_{ij} \cos\theta_{ij}} \tag{46}$$

Total deformation of the entire honeycomb structure in direction-2 under the application of stress σ_2 along the two opposite edges parallel to direction-1 is summation of the individual deformations in direction-2 of n number of strips. Thus

$$\epsilon_2 B = \sum_{j=1}^{n} \epsilon_{2j} B_j \tag{47}$$

By definition of v_{21} Eq. (47) leads to

$$\frac{\epsilon_1}{v_{21eq}} B = \sum_{j=1}^{n} \frac{\epsilon_{1j}}{\hat{v}_{21j}} B_j \tag{48}$$

From the condition of deformation comparability $\epsilon_1 = \epsilon_{1j}$ for $j = 1, 2, \ldots, n$. Thus the equivalent Poisson's ratio for loading direction-2 of the entire irregular honeycomb structure

$$v_{21eq} = \frac{1}{\left(\sum_{j=1}^{n} B_j \frac{\sum_{i=1}^{m} l_{ij} \cos\theta_{ij}}{\sum_{i=1}^{m} v_{21Uij} l_{ij} \cos\theta_{ij}}\right)} \sum_{j=1}^{n} B_j \tag{49}$$

where v_{21Uij} can be obtained from Eq. (43).

It can be noted here that following the similar way as discussed in Section 2.2, the derived expressions of two Poisson's ratios (Eqs. (38) and (49)) can be reduced to the formulae provided by Gibson and Ashby (Gibson and Ashby, 1999) in case of uniform honeycombs (i.e. $B_1 = B_2 = \cdots = B_n$; $s = h/2$; $\alpha = \beta = 90°$; $l_{ij} = l$ and $\theta_{ij} = \theta$, for all i and j), which follows $E_2^* v_{12}^* = E_1^* v_{21}^*$. For regular uniform honeycombs $v_{12}^* = v_{21}^* = 1$, where v_{12}^* and v_{21}^* denote the Poisson's ratios of uniform regular honeycombs.

2.5. Shear modulus (G_{12})

To derive the expression of shear modulus (G_{12U}) for a RUCE, shear stress τ is applied as shown in Fig. 6(a). Lateral deformation of point D with respect to point H consists of three components, namely lateral deformation of the cell wall having inclination angle α, lateral deformation of the vertical cell walls and lateral deformation of the cell wall having inclination angle β. The remaining structure except these two inclined cell walls having inclination angles α and β is symmetric. Thus points A, B, C (and points E, G, F) do not have any relative lateral movement under the applied stresses. For this reason, the cell walls having inclination angle θ do not have any contribution in the lateral deformation of the RUCE. From Fig. 6(b) $M = Fs$, where $F = 2\tau lb\cos\theta$. Due to equal bending stiffness of cell walls AB and BC, they will share half of moment M each. Using the standard result of Euler–Bernoulli beam theory, (deflection at one end due to application of moment at the other end $\delta = Ml^2/6E_sI$), the angle of rotation at joint B can be expressed as

$$\phi = \frac{M}{2} \frac{l}{6E_sI} = \frac{Fsl}{12E_sI} \tag{50}$$

Lateral deformation of the cell wall having inclination angle α has two components, bending deformation and rotational deformation due the rotation of joint B as shown in Fig. 6(b).

Thus the total lateral deformation of point D with respect to point B is

$$\delta_{L1} = \left(\frac{F\sin\alpha}{3EI}\left(\frac{s}{\sin\alpha}\right)^3 + \phi \frac{s}{\sin\alpha}\right)\sin\alpha$$
$$= \frac{Fs^2}{12EI}\left(l + \frac{4s}{\sin\alpha}\right) \tag{51}$$
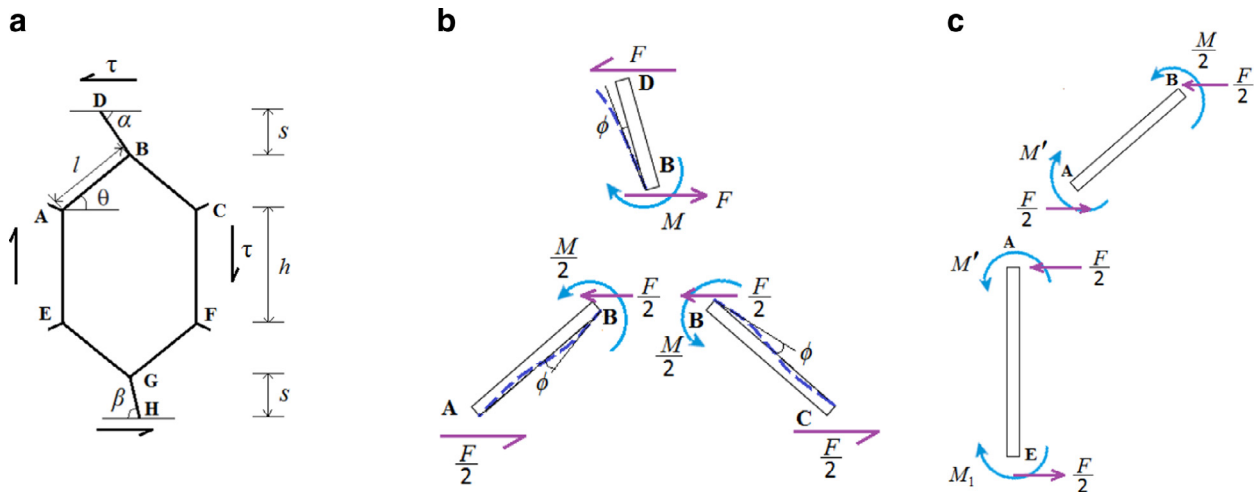

Fig. 6. RUCE and free-body diagram used in the proposed analysis for G_{12}.

Lateral deformation the cell wall having inclination angle β can also be expressed in the similar way as

$$\delta_{L2} = \frac{Fs^2}{12EI}\left(l + \frac{4s}{\sin\beta}\right) \tag{52}$$

In Fig. 6(c), J is the midpoint of the member AE. Displacement of point J with respect to point A is calculated in the similar way as above considering the rotation of point A and bending deformation of member AJ,

$$\delta_{L3} = \frac{Fh^2}{48EI}(l + 2h) \tag{53}$$

Displacement of point J in direction-1 with respect to point E (δ_{L4}) is same as δ_{L3}. By replacing $F = 2\tau lb\cos\theta$ and $I = bt^3/12$ in Eqs. (51)–(53) total lateral movement of point D with respect to point H

$$\delta_L = \delta_{L1} + \delta_{L2} + \delta_{L3} + \delta_{L4}$$
$$= \frac{2\tau l\cos\theta}{Et^3}\left(2ls^2 + h^3 + \frac{h^2 l}{2} + 4s^3\left(\frac{1}{\sin\alpha} + \frac{1}{\sin\beta}\right)\right) \tag{54}$$

The shear strain γ for a RUCE can be expressed as

$$\gamma = \frac{\delta_L}{2s + h + 2l\sin\theta}$$
$$= \frac{2\tau l\cos\theta}{Et^3(2s + h + 2l\sin\theta)}\left(2ls^2 + h^3 + \frac{h^2 l}{2} + 4s^3\left(\frac{1}{\sin\alpha} + \frac{1}{\sin\beta}\right)\right) \tag{55}$$

Thus the expression for shear modulus of a RUCE becomes

$$G_{12U} = \frac{\tau}{\gamma}$$
$$= E_s\left(\frac{t}{l}\right)^3 \frac{(\frac{h}{l} + 2\frac{s}{l} + 2\sin\theta)}{2\cos\theta(2(\frac{s}{l})^2 + 4(\frac{s}{l})^3(\frac{1}{\sin\alpha} + \frac{1}{\sin\beta}) + (\frac{h}{l})^3 + \frac{1}{2}(\frac{h}{l})^2)} \tag{56}$$

To derive the expression of equivalent shear modulus of the entire irregular honeycomb structure (G_{12eq}), the shear moduli for the constituting RUCEs (G_{12U}) are assembled as discussed below. For obtaining G_{12eq}, shear stress τ is applied parallel to direction direction-1 as shown in Fig. 7(a). If the equilibrium of forces for application of stress τ in the jth strip (as highlighted in Fig. 7(b)) is considered,

$$\tau L = \sum_{i=1}^{m} \tau_{ij} L_{ij} \tag{57}$$

By definition of shear modulus Eq. (57) can be rewritten as

$$\hat{G}_{12j}\gamma L = \sum_{i=1}^{m} G_{12Uij}\gamma_{ij}L_{ij} \tag{58}$$

where $\hat{G}_{12j}$ represents the equivalent shear modulus of the jth strip. γ and γ_{ij} are the shear strains of jth strip and individual RUCEs of the jth strip respectively. G_{12Uij} represents the shear modulus of a RUCE positioned at (i, j).

To ensure the deformation compatibility condition $\gamma = \gamma_{ij}$ for $i = 1, 2, \ldots, m$ in the jth strip. Thus Eq. (58) leads to

$$\hat{G}_{12j} = \frac{\sum_{i=1}^{m} G_{12Uij}l_{ij}\cos\theta_{ij}}{\sum_{i=1}^{m} l_{ij}\cos\theta_{ij}} \tag{59}$$

Total lateral deformation of one edge compared to the opposite edge of the entire honeycomb structure under the application of shear stress τ is the summation of the individual lateral deformations of n number of strips. Thus

$$\gamma B = \sum_{j=1}^{n} \gamma_j B_j \tag{60}$$

By definition of G_{12} Eq. (60) leads to

$$\frac{\tau}{G_{12eq}}B = \sum_{j=1}^{n} \frac{\tau_j}{\hat{G}_{12j}}B_j \tag{61}$$

From Eqs. (59) and (61), equivalent shear modulus of the entire irregular honeycomb structure can be expressed as

$$G_{12eq} = \frac{1}{\left(\sum_{j=1}^{n} B_j \frac{\sum_{i=1}^{m} l_{ij}\cos\theta_{ij}}{\sum_{i=1}^{m} G_{12Uij}l_{ij}\cos\theta_{ij}}\right)}\sum_{j=1}^{n} B_j \tag{62}$$

where G_{12Uij} can be obtained from Eq. (56).

It is worthy to note that the derived expression of shear modulus for irregular honeycombs (Eq. (62)) can be reduced to the formulae provided by Gibson and Ashby (Gibson and Ashby, 1999) in case of regular uniform honeycombs (i.e. $B_1 = B_2 = \cdots = B_n$; $s = h/2$; $\alpha = \beta = 90°$; $l_{ij} = l$ and $\theta_{ij} = \theta$, for all i and j) following the similar way as discussed in Section 2.2. For a regular honeycomb with $\theta_{ij} = \theta = 30°$

$$\frac{G_{12}^*}{E_s} = 0.57\left(\frac{t}{l}\right)^3 \tag{63}$$

where G_{12}^* denotes the shear modulus of uniform regular honeycombs. The regular uniform honeycombs correctly obey the relation $G = E/2(1 + \nu)$, where E, G and ν represent Young's modulus, shear modulus and Poisson's ratio of isotropic solids respectively.

(a) Entire idealized irregular honeycomb structure

(b) Idealized j^{th} strip

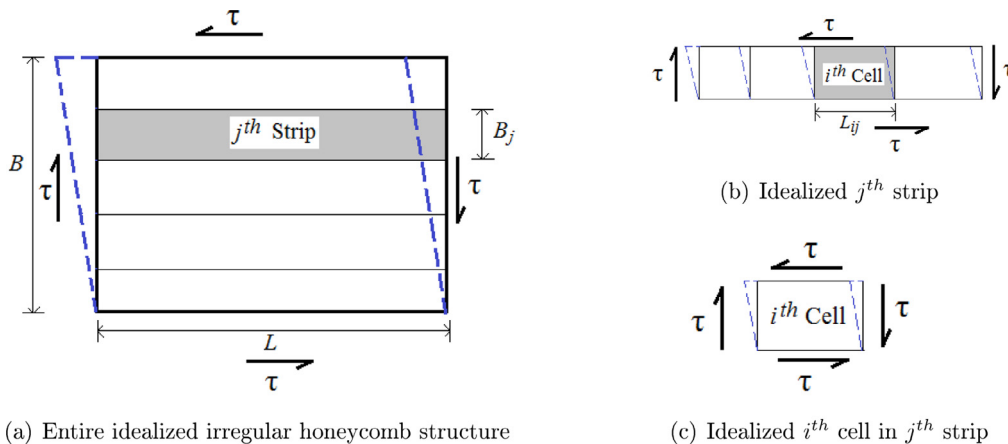(c) Idealized i^{th} cell in j^{th} strip

Fig. 7. Free-body diagrams of idealized irregular honeycomb structure in the proposed analysis of G_{12}.
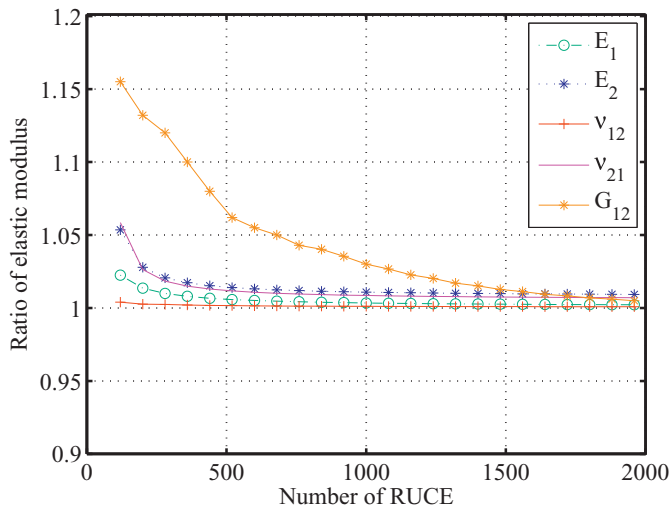
Fig. 8. Convergence study and validation of finite element model for obtaining elastic moduli (Ratio of the elastic moduli obtained using the finite element code and formulae provided by Gibson and Ashby for different elastic moduli have been plotted).

3. Finite element modeling and validation

A finite element code has been developed using Matlab (MATLAB, 2013) to obtain the in-plane elastic moduli numerically for honeycombs having spatially random structural variation. The purpose of the finite element model in the present study is to validate the proposed analytical approach for obtaining in-plane elastic moduli of irregular honeycombs. Each cell wall has been modeled as an Euler–Bernoulli beam element having three degrees of freedom at each node. Axial and shear deformations have been neglected in this study with the assumption of high axial rigidity and low cell wall thickness respectively.

For obtaining E_1 and v_{12} numerically, two opposite edges parallel to direction-2 of the entire honeycomb structure are considered (refer 1). Along one of these two edges, uniform stress parallel to direction-1 is applied while the opposite edge is restrained against translation in direction-1. Remaining two edges (parallel to direction-1) are kept free. Similarly, for obtaining E_2 and v_{21} numerically, two opposite edges parallel to direction-1 of the entire honeycomb structure are considered. Along one of these two edges, uniform stress parallel to direction-2 is applied while the opposite edge is restrained against translation in direction-2. Remaining two edges (parallel to direction-2) are kept free. To obtain G_{12} numerically, uniform shear stress is applied along one edge keeping the opposite edge restrained against translation in direction-1 and 2, while the remaining two edges are kept free.

The finite element model has been validated with results from available literature (Gibson and Ashby, 1999). The developed finite element code is capable of accepting the number of RUCEs in direction-1 and 2 as input in addition to material properties and other geometrical features to obtain corresponding five elastic moduli as output. Representative results for validation are furnished in Fig. 8 for a regular honeycomb having cell angle 30° and h/l ratio of 1.5. Convergence studies have been carried out for the five in-plane elastic moduli with different number of RUCE to ensure the average global behavior of the entire honeycomb by avoiding any localized deformation due to boundary effect. In the present study, the number of RUCE has been adopted as 1681 for all the subsequent analyses.

4. Results and discussions

The analytical approach proposed in this study is capable of obtaining equivalent in-plane elastic properties for irregular honeycombs from known spatial variation of cell angle and material properties of the honeycomb cells. Such irregularities in honeycomb material can be characterized by using common techniques like digital image analysis. For the purpose of finding the range of variation in elastic moduli due to spatial uncertainty, cell angles and material properties can be perturbed following a random distribution within specific bounds. From the expressions of effective elastic moduli derived in Section 2, it is evident that all the five elastic moduli depend on the ratios h/l, t/l, s/l and the angles θ, α, β (refer Fig. 4(a)). In addition to these quantities, the two Young's moduli and shear modulus also depend on E_s. In the present analysis, results (Figs. 10–12) have been presented for three different h/l ratios, namely: 1, 1.5 and 2 with a very small t/l value($\sim 10^{-2}$). For each of these h/l ratios, three different cell angles have been considered, namely: 30°, 45° and 60°. Only bending deformation has been accounted in the present analysis as the effect due to axial and shear deformation becomes negligible for very high axial rigidity and small value of the ratio t/l respectively. In case of large deformation, the axial force that has been neglected in this study, creates a beam-column effect leading to an additional moment in the inclined cell walls caused by the fact that the axial loads no longer remain co-linear. The formulations presented in Section 2 are valid for small strain allowing the non-linearity due to beam-column effect to be neglected. As the two Young's moduli and shear modulus of low density honeycomb are proportional to $E_s \rho^3$ (Zhu et al., 2001), the non-dimensional results for elastic moduli E_1, E_2, v_{12}, v_{21} and G_{12} have been obtained using $\bar{E}_1 = \frac{E_{1eq}}{E_s \rho^3}$, $\bar{E}_2 = \frac{E_{2eq}}{E_s \rho^3}$, $\bar{v}_{12} = v_{12eq}$, $\bar{v}_{21} = v_{21eq}$ and $\bar{G}_{12} = \frac{G_{12eq}}{E_s \rho^3}$ respectively, where '$\bar{\cdot}$' represents the non-dimensional elastic modulus and ρ is the relative density of honeycomb (ratio of the planar area of solid to the total planar area of the honeycomb). Results have been presented for spatial irregularity in the cell angles only. The maximum, minimum and mean values of non-dimensional in-plane elastic moduli for different degree of spatially random variations in cell angles ($\Delta\theta = 0°, 1°, 3°, 5°, 7°$) are shown in Figs. 10–14. For a particular cell angle θ, results have been obtained using a set of uniformly distributed 1000 random samples in the range of $[\theta - \Delta\theta, \theta + \Delta\theta]$. The set of input parameter for a particular sample consists of N number of cell angles in the specified range, where $N(= n \times m)$ is the total number of RUCEs in the entire irregular honeycomb structure. In the present analysis t, s and E_s have been modeled to possess no spatial variation. The quantities h and θ have been considered as the two random input parameters while α, β and l are dependent features. Typical statistical distribution of cell angles for a randomly chosen sample is shown in Fig. 9(a). For that particular sample, the statistical distribution of the inclination angle α is presented in Fig. 9(b). The figures indicate that, even though the cell angles of an irregular honeycomb sample have been drawn from an uniform distribution, interestingly spatial distribution of the inclination angle α changes to Gaussian. The numerical values shown in the right side of each 'I' shaped marks (Figs. 10–14) represent percentage errors in the maximum and minimum values of elastic moduli calculated using the proposed analysis compared to the finite element results. The numerical values shown in the left side represent the same for the mean values. Smaller values in the percentage errors would indicate that the proposed analytical approach is capable of obtaining in-plane elastic moduli for irregular honeycombs with high precision and vice versa. Points on the Y-axis depicts the values of elastic moduli corresponding to perfectly periodic cell structure (i.e.$\Delta\theta = 0$).
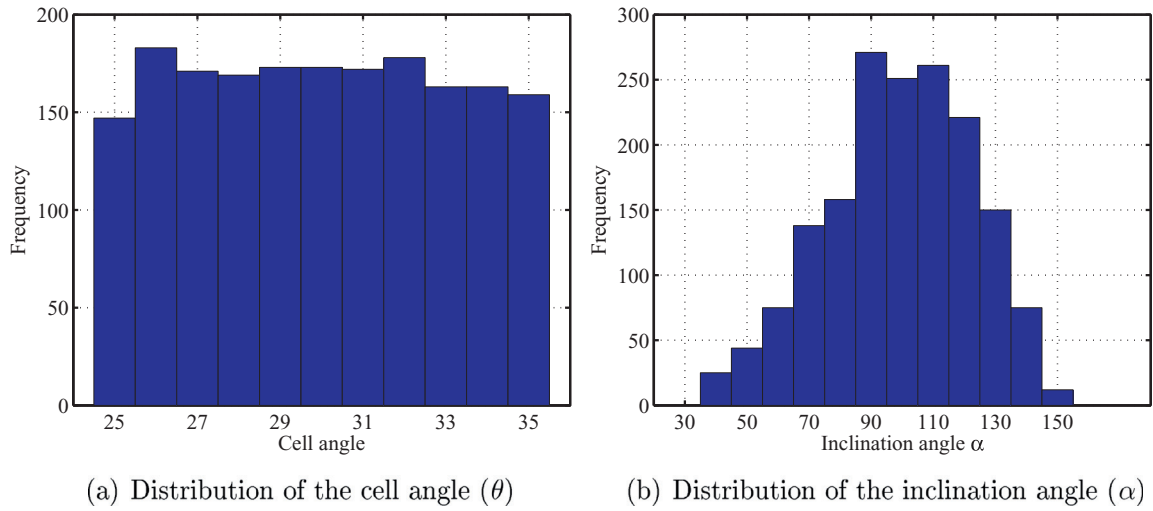
(a) Distribution of the cell angle (θ)

(b) Distribution of the inclination angle (α)

Fig. 9. Typical statistical distribution of cell angle (θ) and inclination angle α (number of RUCE: 1681).
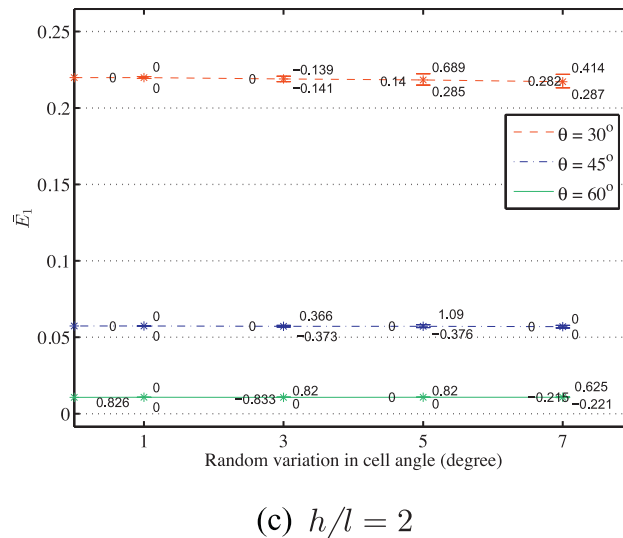
(a) $h/l = 1$

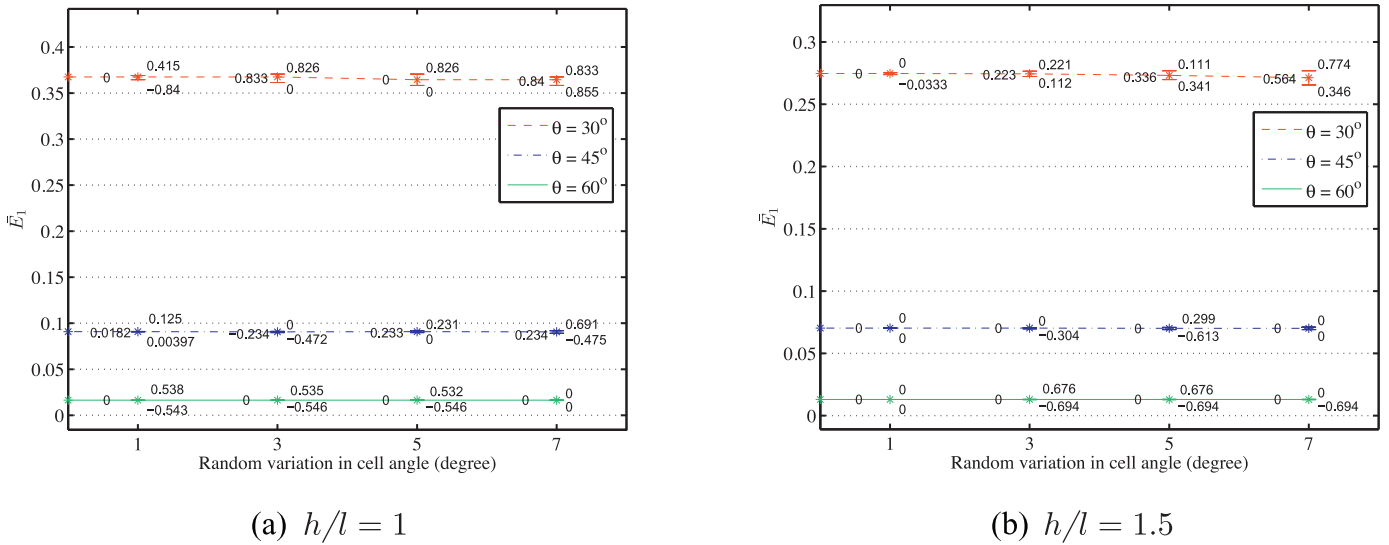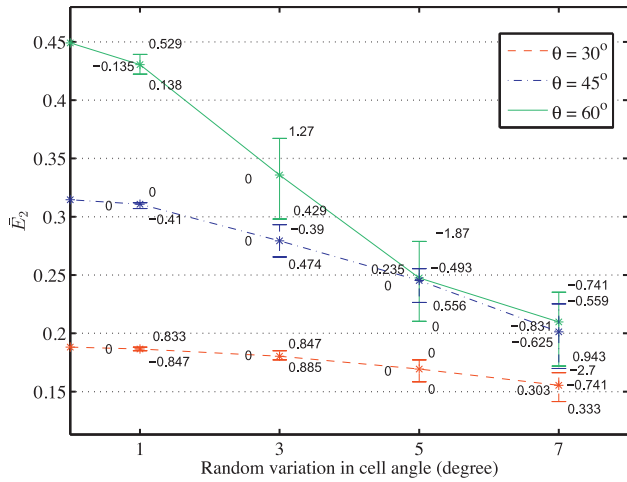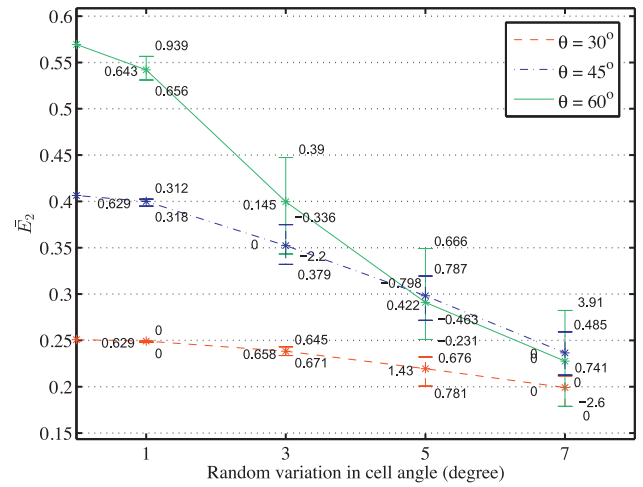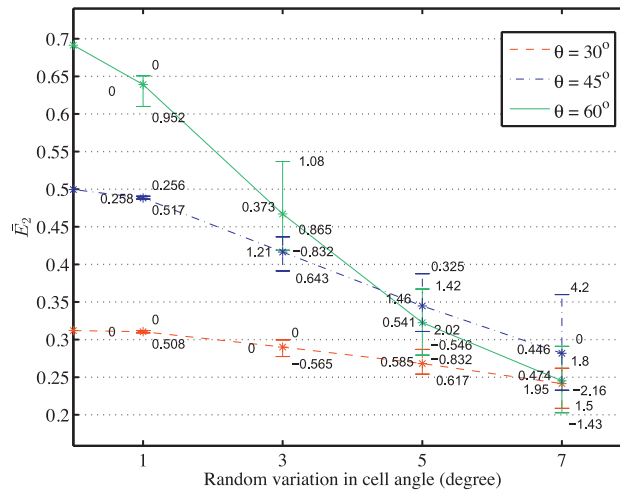(b) $h/l = 1.5$

(c) $h/l = 2$

Fig. 10. Effect of structural irregularity on non-dimensional E_1.

(a) $h/l = 1$

(b) $h/l = 1.5$

(c) $h/l = 2$

Fig. 11. Effect of structural irregularity on non-dimensional E_2.

4.1. Longitudinal elastic modulus (E_1)

Variation in the values of E_1 due to spatially random variations in the cell angles is shown in Fig. 10. From the figures it is clear that irregularity in the cell angles have negligible influence in the longitudinal elastic modulus. Fig. 10 also reveals that with the increase of both the cell angle (θ) and h/l ratio, the mean values of non-dimensional E_1 for the entire irregular honeycomb decrease. This can be attributed to the fact that same trend is followed in the non-dimensional E_1 of a single RUCE with the variation of cell angle and h/l ratio.

4.2. Transverse elastic modulus (E_2)

Fig. 11 shows the effect of irregularity due to spatially random variations of cell angles in E_2. From the figures it is evident that the values of E_2 reduce considerably with increasing degree of random variations in cell angles. The highest rate of reduction in the values of E_2 with the increase in degree of irregularity is noticed

for mean cell angle of 60°, followed by 45° and 30°. Fig. 11 also reveals that with the increase of both cell angle (θ) and h/l ratio, mean values of non-dimensional E_2 for the entire irregular honeycomb increase depending on the variation of non-dimensional E_2 of a single RUCE with cell angle and h/l ratio respectively. The range of variation of E_2 is found to increase with increasing degree of irregularity in cell angles.

4.3. Poisson's ratio ν_{12}

Variation of ν_{12} due to spatially random variations in cell angles is shown in Fig. 12. The figures indicate that irregularity in cell angles do not have much influence in ν_{12}. The highest reduction in the values of ν_{12} with the increase in degree of irregularity is noticed for mean cell angle of 30°. Fig. 12 also shows that with the increase of both cell angle (θ) and h/l ratio, mean values of ν_{12} for the entire irregular honeycomb decrease depending on the variation of ν_{12} of a single RUCE with cell angle and h/l ratio respectively.
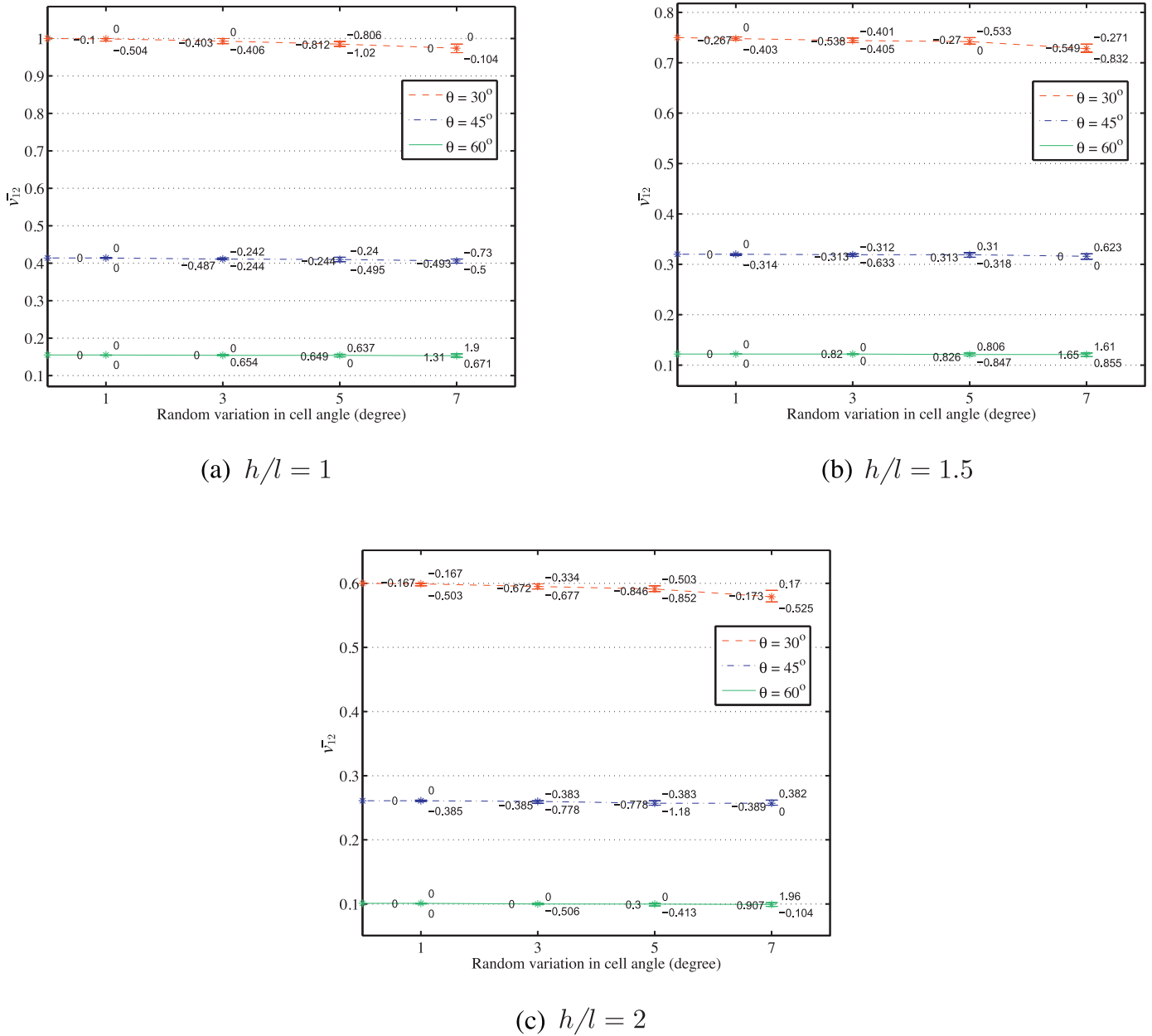
(a) $h/l = 1$

(b) $h/l = 1.5$

(c) $h/l = 2$

Fig. 12. Effect of structural irregularity on non-dimensional ν_{12}.

4.4. Poisson's ratio ν_{21}

Fig. 13 shows the effect of irregularity due to spatially random variations of cell angles in ν_{21}. From the figures it is evident that the values of ν_{21} reduce considerably with increasing degree of random variations in cell angles. The highest rate of reduction in the values of ν_{21} with the increase in degree of irregularity is noticed for mean cell angle of 60°, followed by 45° and 30°. Fig. 13 also reveals that with the increase of both cell angle (θ) and h/l ratio, mean values of non-dimensional ν_{21} for the entire irregular honeycomb increase depending on the variation of ν_{21} of a single RUCE with cell angle and h/l ratio respectively.

4.5. Shear modulus (G_{12})

The effect of irregularity due to spatially random variations of cell angles in G_{12} is depicted in Fig. 14, which shows that the values of G_{12} reduce considerably with increasing degree of

random variations in cell angles. Fig. 14 also reveals that with the increase of both cell angle (θ) and h/l ratio, mean values of non-dimensional G_{12} for the entire irregular honeycomb decrease depending on the variation of G_{12} of a single RUCE with cell angle and h/l ratio respectively. The range of variation of non-dimensional G_{12} is noticed to increase with increasing degree of spatially random variations in cell angle.

4.6. Discussion

The results presented in Sections 4.1–4.5 show that the elastic moduli obtained using the analytical method and by finite element simulation are in good agreement, establishing the validity of the closed-form expressions derived here. Papka and Kyriakides (1994) have reported that under-expansion in honeycomb cells results in a response which has a higher elastic moduli, while over-expansion has the opposite effect. The present investigation shows the effects of spatially random distribution of under and over expanded cells
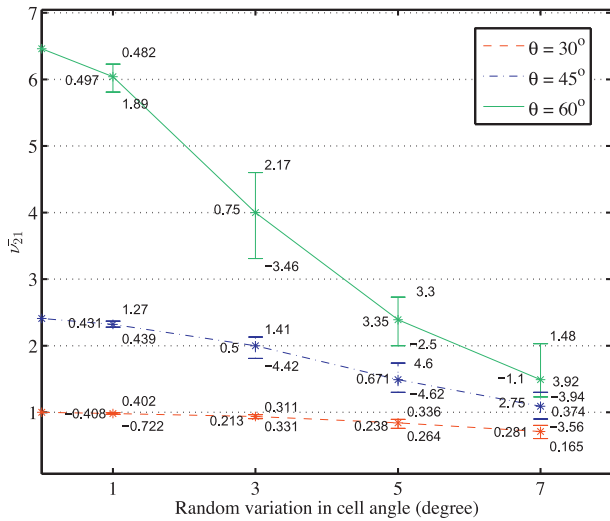
(a) $h/l = 1$
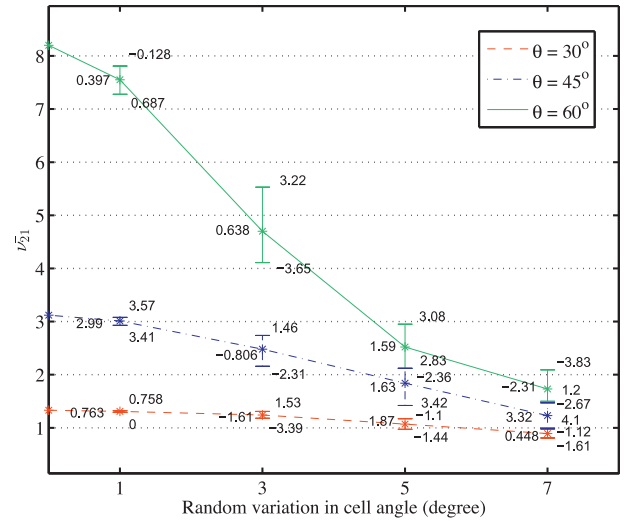
(b) $h/l = 1.5$
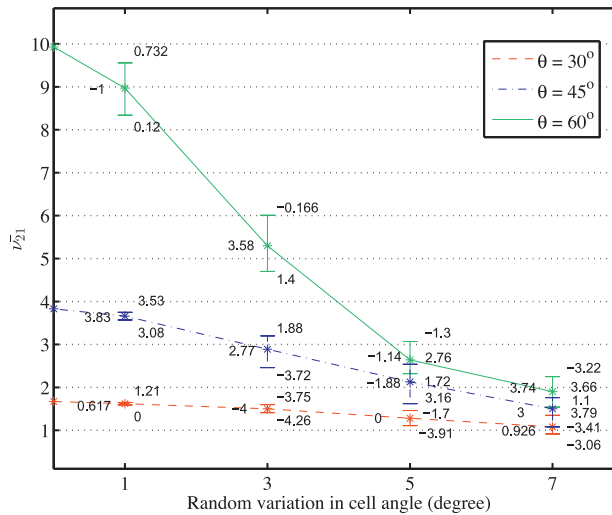
(c) $h/l = 2$

Fig. 13. Effect of structural irregularity on non-dimensional ν_{21}.

of different degree on elastic moduli of the entire irregular honey-comb structure. Fig. 10–14 show that the variation in E_1 and ν_{12} due to spatially random variations in cell angles is very less, while there is considerable amount of reductions in the values of E_2, ν_{21} and G_{12} with increasing degree of irregularity. In the analysis of irregular honeycomb structure having spatially random variations in cell angles, the cell walls having inclination angles α and β play a vital role. As the range of random variation in cell angles ($\Delta\theta$) increases, the inclination angle with respect to direction-2 of these cell walls are also found to increase. Thus with the increase of $\Delta\theta$, component of axial stiffness of these cell walls in direction-1 increase, while that in direction-2 decrease. As the cell walls are considered axially rigid in this analysis, component of axial stiffness of these cell walls in direction-2 are much higher compared to bending stiffness for small value of $\Delta\theta$. Thus with the increase of $\Delta\theta$, stiffness in direction-2 decreases causing subsequent reduction in E_2 and ν_{21}. However for small $\Delta\theta$ as considered in this study, component of axial stiffness of these cell walls in direction-

1 are much lesser compared to that of direction-2 resulting the bending stiffness to be predominant in direction-1. Due to this reason, the variations in E_1 and ν_{12} are found negligible for small $\Delta\theta$. The reason for reduction in G_{12} with the increase of $\Delta\theta$ can be explained using the same analogy. Under the application of shearing stresses (refer Fig. 7(a)), as the component of bending stiffness in direction-1 decreases with the increase with $\Delta\theta$, a subsequent reduction in reduction in G_{12} is noticed.

5. Summary and conclusions

A novel analytical approach for predicting equivalent in-plane elastic moduli of honeycombs having spatial irregularities is presented in this article. Though there are few literature available dealing with different forms of irregularity in honeycombs, those are based on either experimental investigation or numerical simulation approach. This study proposes an efficient analytical framework. The results obtained using the proposed analytical method
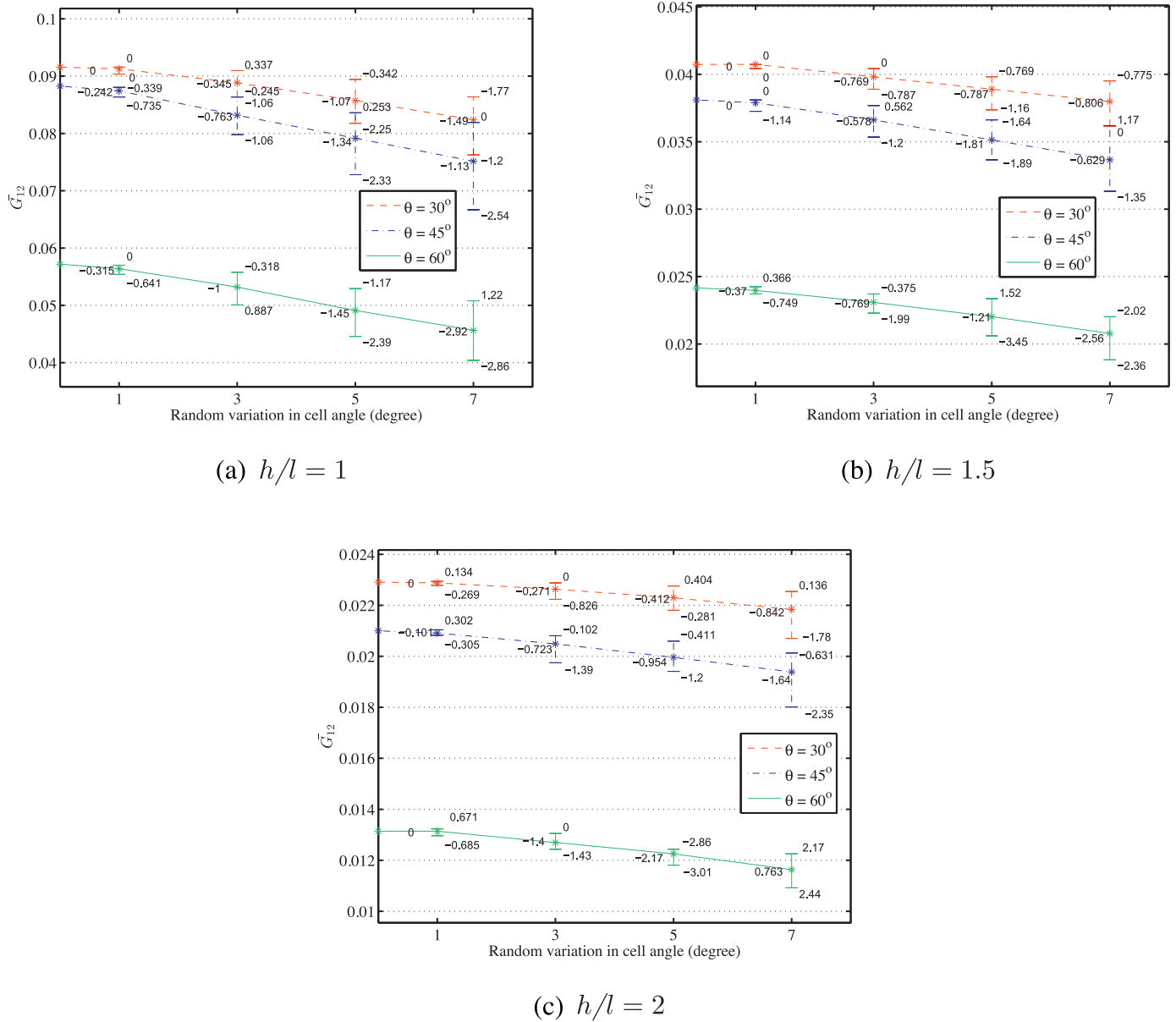
(a) $h/l = 1$

(b) $h/l = 1.5$

(c) $h/l = 2$

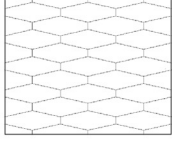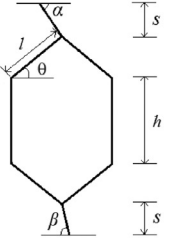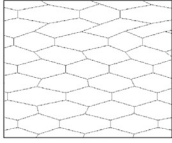**Fig. 14.** Effect of structural irregularity on non-dimensional G_{12}.

for spatially random variation of cell angles have been compared with those obtained from the direct finite element simulation. The mean and range of variation for different elastic moduli are found to be in good agreement. Equivalent elastic properties of irregular honeycombs can be obtained using the proposed analytical framework more efficiently compared to expensive finite element simulation approach without compromising the accuracy of results. The closed-form formulae of elastic moduli for irregular honeycombs have been summarized in Table 1 for ready reference to the readers along with the expressions of elastic moduli for uniform honeycombs. The quantities Z_{GA}, Z_U and Z_{eq} represent the elastic moduli of regular honeycomb provided by Gibson and Ashby (Gibson and Ashby, 1999), elastic moduli of a single representative unit cell element (RUCE) and elastic moduli of the entire irregular honeycomb respectively, where 'Z' denotes the in-plane elastic modulus.

It can be noticed that the expressions of longitudinal Young's modulus, transverse Young's modulus and shear modulus are functions of both structural geometry and material properties of the

irregular honeycomb (i.e. ratios h/l, t/l, s/l and angles θ, α, β and E_s), while the Poisson's ratios depend only on structural geometry of irregular honeycombs (i.e. ratios h/l, t/l, s/l and angles θ, α, β) (refer Table 1).

An important finding of this study is that, though the effect of variations in cell angle on E_1 and ν_{12} is small, E_2, ν_{21} and G_{12} reduce significantly with the increase in degree of random variation of the cell angles. The highest reduction in the values of elastic moduli is observed in case of E_2 and ν_{21}, when the mean cell angle is considered $60°$. This uncertainty in the elastic moduli of honeycombs owing to random variations in cell angle would have significant influence on the subsequent analysis and design process. The formulae developed here can also be used to predict equivalent in-plane elastic moduli of irregular honeycombs having spatial variation in material properties and thickness of cell wall. The proposed conceptual analytical framework to efficiently deal with spatial irregularities in honeycombs can be extended further to other cellular structures considering appropriate representative unit cell element.

Table 1
Summary of formulae for effective in-plane elastic properties of honeycombs.

Parameter / Structural configuration	In-plane elastic properties				
	E_1	E_2	ν_{12}	ν_{21}	G_{12}
Regular honeycomb	$E_{1GA} = E_s\left(\frac{t}{l}\right)^3 \dfrac{\cos\theta}{(\frac{h}{l}+\sin\theta)\sin^2\theta}$	$E_{2GA} = E_s\left(\frac{t}{l}\right)^3 \dfrac{(\frac{h}{l}+\sin\theta)}{\cos^3\theta}$	$\nu_{12GA} = \dfrac{\cos^2\theta}{(\frac{h}{l}+\sin\theta)\sin\theta}$	$\nu_{21GA} = \dfrac{(\frac{h}{l}+\sin\theta)\sin\theta}{\cos^2\theta}$	$G_{12GA} = E_s\left(\frac{t}{l}\right)^3 \dfrac{(\frac{h}{l}+\sin\theta)}{(\frac{h}{l})^2(1+2\frac{h}{l})\cos\theta}$
Representative unit cell element (RUCE)	$E_{1U} = E_s\left(\frac{t}{l}\right)^3 \dfrac{\cos\theta}{(\frac{h}{l}+\sin\theta)\sin^2\theta}$	$E_{2U} = E_s\left(\frac{t}{l}\right)^3 \dfrac{\left(\frac{h}{l}+2\frac{s}{l}+2\sin\theta\right)}{\cos\theta\left(2\cos^2\theta+8\left(\frac{s}{l}\right)^3\left(\frac{\cos^2\alpha}{\sin^3\alpha}+\frac{\cos^2\beta}{\sin^3\beta}\right)+2\left(\frac{s}{l}\right)^2(\cot^2\alpha+\cot^2\beta)\right)}$	$\nu_{12U} = \dfrac{2\cos^2\theta}{\left(2\sin\theta+2\frac{s}{l}+\frac{h}{l}\right)\sin\theta}$	$\nu_{21U} = \dfrac{\sin\theta\left(\frac{h}{l}+2\frac{s}{l}+2\sin\theta\right)}{2\cos^2\theta+8\left(\frac{s}{l}\right)^3\left(\frac{\cos^2\alpha}{\sin^3\alpha}+\frac{\cos^2\beta}{\sin^3\beta}\right)+2\left(\frac{s}{l}\right)^2(\cot^2\alpha+\cot^2\beta)}$	$G_{12U} = E_s\left(\frac{t}{l}\right)^3 \dfrac{\left(2\frac{s}{l}+\frac{h}{l}+2\sin\theta\right)}{2\cos\theta\left(2\left(\frac{s}{l}\right)^2+4\left(\frac{s}{l}\right)^3\left(\frac{1}{\sin\alpha}+\frac{1}{\sin\beta}\right)+\frac{1}{2}\left(\frac{h}{l}\right)^3+\left(\frac{s}{l}+\sin\theta\right)\left(\frac{h}{l}\right)^2\right)}$
Irregular honeycomb	$E_{1eq} = \dfrac{1}{\sum_{j=1}^{n}B_j}\sum_{j=1}^{n}\left(\dfrac{\sum_{i=1}^{m}l_{ij}\cos\theta_{ij}}{\sum_{i=1}^{m}\frac{l_{ij}\cos\theta_{ij}}{E_{1Uij}}}\right)B_j$	$E_{2eq} = \dfrac{1}{\sum_{j=1}^{n}B_j}\sum_{j=1}^{n}\left(\dfrac{\sum_{i=1}^{m}l_{ij}\cos\theta_{ij}}{\sum_{i=1}^{m}E_{2Uij}l_{ij}\cos\theta_{ij}}\right)B_j$	$\nu_{12eq} = \dfrac{1}{\sum_{j=1}^{n}B_j}\sum_{j=1}^{n}\left(\dfrac{\sum_{i=1}^{m}l_{ij}\cos\theta_{ij}}{\sum_{i=1}^{m}\frac{l_{ij}\cos\theta_{ij}}{\nu_{12Uij}}}\right)B_j$	$\nu_{21eq} = \dfrac{1}{\sum_{j=1}^{n}B_j}\sum_{j=1}^{n}\left(\dfrac{\sum_{i=1}^{m}l_{ij}\cos\theta_{ij}}{\sum_{i=1}^{m}\nu_{21Uij}l_{ij}\cos\theta_{ij}}\right)B_j$	$G_{12eq} = \dfrac{1}{\sum_{j=1}^{n}B_j}\sum_{j=1}^{n}\left(\dfrac{\sum_{i=1}^{m}l_{ij}\cos\theta_{ij}}{\sum_{i=1}^{m}G_{12Uij}l_{ij}\cos\theta_{ij}}\right)B_j$

References

Ajdari, A., Jahromi, B.H., Papadopoulos, J., Nayeb-Hashemi, H., Vaziri, A., 2012. Hierarchical honeycombs with tailorable properties. Int. J. Solids Struct. 49 (11–12), 1413–1419.

Ajdari, A., Nayeb-Hashemi, H., Canavan, P., Warner, G., 2008. Effect of defects on elastic-plastic behavior of cellular materials. Mater. Sci. Eng. A 487 (1–2), 558–567.

Basaruddin, K.S., Kamarrudin, N.S., Ibrahim, I., 2014. Stochastic multi-scale analysis of homogenised properties considering uncertainties in cellular solid microstructures using a first-order perturbation. Latin Am. J. Solids Struct. 11 (5), 755–769.

Chen, D.H., Yang, L., 2011. Analysis of equivalent elastic modulus of asymmetrical honeycomb. Compos. Struct. 93 (2), 767–773.

Critchley, R., Corni, I., Wharton, J.A., Walsh, F.C., Wood, R.J.K., Stokes, K.R., 2013. A review of the manufacture, mechanical properties and potential applications of auxetic foams. Phys. Status Solidi B 250 (10), 1963–1982.

Dey, S., Mukhopadhyay, T., Khodaparast, H.H., Adhikari, S., 2015. Stochastic natural frequency of composite conical shells. Acta Mechanica 226, 2537–2553.

Dey, S., Mukhopadhyay, T., Khodaparast, H.H., Kerfriden, P., Adhikari, S., 2015. Rotational and ply-level uncertainty in response of composite shallow conical shells. Compos. Struct. 131, 594–605.

Dey, S., Mukhopadhyay, T., Sahu, S.K., Li, G., Rabitz, H., Adhikari, S., 2015. Thermal uncertainty quantification in frequency responses of laminated composite plates. Compos. Part Eng. 80, 186–197.

El-Sayed, F.K.A., Jones, R., Burgess, I.W., 1979. A theoretical approach to the deformation of honeycomb based composite materials. Composites 10 (4), 209–214.

Gibson, L., Ashby, M.F., 1999. Cellular Solids Structure and Properties. Cambridge University Press, Cambridge, UK.

Goswami, S., 2006. On the prediction of effective material properties of cellular hexagonal honeycomb core. J. Reinf. Plast. Compos. 25 (4), 393–405.

Hu, L.L., Yu, T.X., 2013. Mechanical behavior of hexagonal honeycombs under low-velocity impact- theory and simulations. Int. J. Solids Struct. 50 (20–21), 3152–3165.

Hurtado, J.E., Barbat, A.H., 1998. Monte carlo techniques in computational stochastic mechanics. Arch. Comput. Methods Eng. 5 (1), 3–29.

Jang, W.Y., Kyriakides, S., 2015. On the buckling and crushing of expanded honeycomb. Int. J. Mech. Sci. 91, 81–90.

Klintworth, J.W., Stronge, W.J., 1988. Elasto-plastic yield limits and deformation laws for transversely crushed honeycombs. Int. J. Mech. Sci. 30 (3–4), 273–292.

Li, K., Gao, X.L., Subhash, G., 2005. Effects of cell shape and cell wall thickness variations on the elastic properties of two-dimensional cellular solids. Int. J. Solids Struct. 42 (5–6), 1777–1795.

Li, K., Gao, X.L., Wang, J., 2007. Dynamic crushing behavior of honeycomb structures with irregular cell shapes and non-uniform cell wall thickness. Int. J. Solids Struct. 44 (14-15), 5003–5026.

Liu, W., Wang, N., Huang, J., Zhong, H., 2014. The effect of irregularity, residual convex units and stresses on the effective mechanical properties of 2d auxetic cellular structure. Mater. Sci. Eng. A 609, 26–33.

Liu, Y., Xie, B., Zhang, Z., Zheng, Q., Xu, Z., 2012. Mechanical properties of graphene papers. J. Mech. Phys. Solids 60 (4), 591–605.

Lopez Jimenez, F., Triantafyllidis, N., 2013. Buckling of rectangular and hexagonal honeycomb under combined axial compression and transverse shear. Int. J. Solids Struct. 50 (24), 3934–3946.

MATLAB, 2013. MATLAB version 8.2.0.701 (R2013b) . The MathWorks Inc..

Mousanezhad, D., Ebrahimi, H., Haghpanah, B., Ghosh, R., Ajdari, A., Hamouda, A. M. S., Vaziri, A.,. 2015. Spiderweb honeycombs.Int. J. Solids Struct.. doi: http://dx.doi.org/10.1016/j.ijsolstr.2015.03.036.

Pantano, A., Parks, D.M., Boyce, M.C., 2004. Mechanics of deformation of single- and multi-wall carbon nanotubes. J. Mech. Phys. Solids 52 (4), 591–605.

Papka, S.D., Kyriakides, S., 1994. In-plane compressive response and crushing of honeycomb. J. Mech. Phys. Solids 42 (10), 1499– 1532.

Papka, S.D., Kyriakides, S., 1998. Experiments and full-scale numerical simulations of in-plane crushing of a honeycomb. Acta Materialia 46 (8), 2765– 2776.

Roark, R.J., Young, W.C., 1976. Formulas for Stress and Strain. McGraw-Hill Book Company.

Rossiter, J., Takashima, K., Scarpa, F., Walters, P., Mukai, T., 2014. Shape memory polymer hexachiral auxetic structures with tunable stiffness. Smart Mater. Struct. 23 (4), 045007.

Scarpa, F., Adhikari, S., Phani, A.S., 2009. Effective elastic mechanical properties of single layer graphene sheets. Nanotechnology 20 (6), 5709.

Scarpa, F., Panayiotou, P., Tomlinson, G., 2000. Numerical and experimental uniaxial loading on in-plane auxetic honeycombs. J. Strain Anal. Eng. Des. 35 (5), 383–388.

Schaeffer, M., Ruzzene, M., 2015. Wave propagation in multistable magneto-elastic lattices. Int. J. Solids Struct. 56–57, 78– 95. http://dx.doi.org/10.1016/j.ijsolstr.2014.12.003.

Triantafyllidis, N., Schraad, M.W., 1998. Onset of failure in aluminum honeycombs under general in-plane loading. J. Mech. Phys. Solids 46 (6), 1089– 1124.

Warren, W.E., Kraynik, A.M., 1987. Foam mechanics: the linear elastic response of two-dimensional spatially periodic cellular materials. Mech. Mater. 6 (1), 27–37.

Warren, W.E., Kraynik, A.M., Stone, C.M., 1989. A constitutive model for two-dimensional nonlinear elastic foams. J. Mech. Phys. Solids 37 (6), 717– 733.

Wilbert, A., Jang, W.Y., Kyriakides, S., Floccari, J.F., 2011. Buckling and progressive crushing of laterally loaded honeycomb. Int. J. Solids Struct. 48 (5), 803– 816.

Yongqiang, L., Zhiqiang, J., 2008. Free flexural vibration analysis of symmetric rectangular honeycomb panels with SCSC edge supports. Compos. Struct. 83 (2), 154–158.

Zenkert, D., 1995. An Introduction to Sandwich Construction. Chameleon Press, London.

Zhang, J., Ashby, M.F., 1992. The out-of-plane properties of honeycombs. Int. J. Mech. Sci. 34 (6), 475–489.

Zhu, H.X., Hobdell, J.R., Miller, W., Windle, A.H., 2001. Effects of cell irregularity on the elastic properties of 2D Voronoi honeycombs. J. Mech. Phys. Solids 49 (4), 857–870.

Zhu, H.X., Thorpe, S.M., Windle, A.H., 2006. The effect of cell irregularity on the high strain compression of 2D Voronoi honeycombs. Int. J. Solids Struct. 43 (5), 1061–1078.